

Polyfunctional Phosphine Ligands. Synthesis of 7-Diphenylphosphino-2,4-dimethyl-1,8-naphthyridine and its Co-ordination Properties †

Maria Grassi,^a Giovanni De Munno,^b Francesco Nicolò^c and Sandra Lo Schiavo^{*,c}

^a Dipartimento di Chimica Inorganica e Metallorganica, Università di Milano, Via Venezian 21, I-20133 Milano, Italy

^b Dipartimento di Chimica, Università della Calabria, 87030 Arcavacata di Rende, Cosenza, Italy

^c Dipartimento di Chimica Inorganica e Struttura Molecolare, Università di Messina, Salita Sperone n.31, Vill. S. Agata, 98010 Messina, Italy

The new trinucleating ligand 7-diphenylphosphino-2,4-dimethyl-1,8-naphthyridine (dpnapy) has been prepared and its co-ordination chemistry with rhodium(I) complexes investigated. Reactions with $[\{\text{Rh}(\text{cod})\text{Cl}\}_2]$ (cod = cycloocta-1,5-diene) lead to different products depending on the ligand to metal ratio. The P-monodentate ligand complex $[\text{Rh}(\text{cod})(\text{dpnapy})\text{Cl}]$ **1** is formed when a 2:1 ligand:dimer ratio is used. The cod region of the ¹H and ¹³C NMR spectra of **1** is temperature dependent. The fluxional behaviour can be explained by the formation of a five-co-ordinate intermediate displaying rapid intramolecular exchange of the cod olefinic and CH₂ protons. A lower activation energy process, not frozen at 215 K, is also observed. At room temperature (r.t.) the two-dimensional ¹H and ³¹P chemical exchange spectra indicate a further slower dynamic equilibrium $\mathbf{1} \rightleftharpoons \mathbf{2}$ with loss of dpnapy. The binuclear complex $[\{\text{Rh}(\text{cod})\text{Cl}\}_2(\mu\text{-dpnapy})]$ **2**, in which dpnapy acts as bridging bidentate ligand using the phosphorus and the terminal nitrogen atoms, is the reaction product when a 1:1 ligand:dimer ratio is used. The ¹H and ¹³C NMR data for complex **2** are consistent with a dimeric structure of low symmetry. Complex **2** is also involved in several dynamic processes. At r.t. the two-dimensional ¹H chemical exchange spectrum shows a slow general scrambling of the cod olefinic protons and the presence of the equilibrium $\mathbf{2} \rightleftharpoons \mathbf{1}$ with participation of $[\{\text{Rh}(\text{cod})\text{Cl}\}_2]$. The ligand reacts with $[\{\text{Rh}(\text{CO})_2\text{Cl}\}_2]$ giving as the only isolable product the metallocycle $[\{\text{Rh}(\text{CO})(\mu\text{-dpnapy})\text{Cl}\}_2] \cdot 2\text{CH}_2\text{Cl}_2$ **3**. The reaction proceeds through several steps involving the formation of *cis*-dicarbonyl intermediates as indicated by IR and NMR spectra. The structure of **3** has been determined by X-ray crystallography. It consists of two Rh(CO)Cl units, joined together by two dpnapy molecules in a head-to-tail arrangement.

In the last decade polydentate ligands capable of producing linear chains or more complex arrays of metal centres have been the subject of considerable interest. Much of this attention was focused on short-bite polyfunctional phosphines. Balch and co-workers have demonstrated the usefulness of ligands such as bis(diphenylphosphinomethyl)phenylphosphine¹ and 2,6-bis(diphenylphosphino)pyridine as building blocks for linear arrays of three or four rhodium atoms as well as the capacity of bis(diphenylphosphinomethyl)phenylarsine in the construction of metallomacrocycles.² Furthermore the presence in the metallomacrocyclic of both Lewis-acid and -base sites allows the complexation of a large variety of metal ions³ in the central cavity. For example the complex $[\text{Ir}_2\{\mu\text{-(Ph}_2\text{PCH}_2)_2\text{AsPh}\}_2(\text{CO})_2\text{Cl}_2]$ co-ordinates transition-metal ions (Ag⁺, Cu⁺, etc.) through the two arsenic sites and s² main-group ions (Pb²⁺, Tl⁺, etc.) through the iridium centres. These last adducts are of particular interest because they show intense absorptions in the visible spectra and strong photoluminescence.

Following our interest in the synthesis and chemical properties of bi- and poly-nuclear complexes⁴ we have focused our attention on polynucleating ligands able to promote either the formation of polynuclear linear-chain metal complexes or the formation of metallomacrocycles. In this context we have designed two new polyfunctional phosphines, the 7-diphenylphosphino-2,4-dimethyl-1,8-naphthyridine and 2,7-bis-

(diphenylphosphino)-4-methyl-1,8-naphthyridine, that can be regarded as a combination of the short-bite ligands, 1,8-naphthyridine and 2-(diphenylphosphino)pyridine. The co-ordination chemistry of 1,8-naphthyridine has been widely studied in relation to a variety of metals displaying various geometries ranging from monodentate, chelating bidentate to bridging bidentate.⁵ Its ability to act in a bridging bidentate mode has been facilitated by adding functional groups in position 2, or in positions 2 and 7.⁶ A naphthyridine derivative, the 1,8-naphthyridin-2-one anion,⁷ has been used to promote the formation of rhodium trinuclear complexes. On the other hand, 2-(diphenylphosphino)pyridine is one of the most studied bidentate ligands and its ability to act as a bridging hetero-binucleating entity is amply demonstrated.^{4b-d,8}

In this paper we report the synthesis and the NMR characterization of the new trinucleating ligand 7-diphenylphosphino-2,4-dimethyl-1,8-naphthyridine (dpnapy) and of some rhodium(I) complexes containing it. The NMR-based structural and dynamic characterization of the latter is also illustrated. Finally we report the X-ray analysis of the metallocycle $[\{\text{Rh}(\text{CO})(\mu\text{-dpnapy})\text{Cl}\}_2] \cdot 2\text{CH}_2\text{Cl}_2$.

Experimental

General Data.—The starting materials $[\{\text{Rh}(\text{cod})\text{Cl}\}_2]$ ⁹ (cod = cycloocta-1,5-diene), $[\{\text{Rh}(\text{CO})_2\text{Cl}\}_2]$ ¹⁰ and 7-chloro-2,4-dimethyl-1,8-naphthyridine¹¹ (cnapy) were prepared according to the literature methods. The other reagents were commercially obtained and used as supplied. All reactions were carried out

† Supplementary data available: see Instructions for Authors, *J. Chem. Soc., Dalton Trans.*, 1992, Issue 1, pp. xx–xxv.

under an atmosphere of nitrogen. Tetrahydrofuran (thf) was distilled by a standard procedure. Infrared spectra were recorded on KBr or CsI pellets with a Perkin Elmer FT 1720X spectrometer, NMR spectra on Bruker AC-200 and Varian XL-200 spectrometers using standard pulse sequences.¹² Mixing times of 1 and 0.5 s were used in the two-dimensional ³¹P nuclear Overhauser effect (NOESY) and ¹H chemical exchange (NOESYPH) spectra. Inverse ¹³C-¹H two-dimensional correlation (pulse sequence BIRDREV) spectra were measured on a Bruker AC-200 instrument equipped with a second synthesizer for the X frequency generation (B-SV 3 unit); a 5 mm probe head with ¹H inner coil and tuneable outer coil was employed. Solvents and temperatures are given in Tables 1–3. Conductivity data were obtained with a Radiometer CDM 3 conductivity meter. Molecular weights were determined with a Knauer vapour-pressure osmometer. Elemental analyses were performed by Malissa-Reuter Mikroanalytisches Laboratorium, Elbach, Germany, and by the Microanalytical Laboratory of the Organic Chemistry Institute of Milan.

Preparations.—7-Diphenylphosphino-2,4-dimethyl-1,8-naphthyridine. A hexane solution of *n*-butyllithium (1.6 mol dm⁻³, 8.19 cm³) was added to a freshly distilled thf solution (120 cm³) of PPh₂H (2.44 g, 0.013 mol). The resulting orange mixture was left to stir for about 15 min and then solid 7-chloro-2,4-dimethyl-1,8-naphthyridine (2.5 g, 0.0129 mol) was added in small amounts over 0.5 h. Upon addition of cnapy the starting orange solution immediately turned dark red-violet. After stirring (4 h) the solvent was removed *in vacuo* leaving a dark red oil. This was dissolved in dichloromethane (20 cm³) and the resulting solution passed through a silica gel (70–230 mesh) column (2 × 20 cm³) saturated with the same solvent. Elution by CH₂Cl₂-hexane (1:1) gave a yellow fraction from which, by removal of the solvent, a yellow oily powder containing the product was obtained. By recrystallization from CH₂Cl₂-hexane (1:3) (60 cm³) at -20 °C the pure compound was obtained as white microcrystals, m.p. 152.4 °C (yield 2.44 g, 55%) (Found: C, 77.25; H, 5.60; N, 8.20; P, 9.00. Calc. for C₂₂H₁₆N₂P: C, 77.15; H, 5.60; N, 8.20; P, 9.05%). IR (Nujol, KBr): ν_{max} 1610, 1580, 1536, 1495, 807, 765, 749, 731, 727 and 493 cm⁻¹.

[Rh(cod)(dpnapy)Cl] **1**. **Procedure (a)**. A solution of dpnapy (0.070 g, 0.203 mmol) and [Rh(cod)Cl]₂ (0.050 g, 0.101 mmol) in CH₂Cl₂ (30 cm³) was stirred for about 10 min. Then hexane was added inducing the precipitation of compound **1** as a yellow solid. It was washed with diethyl ether and dried *in vacuo*. Yield 88% (0.105 g, 0.178 mmol).

Procedure (b). Solid dpnapy (0.021 g, 0.06 mmol) was added to a dichloromethane solution (30 cm³) of [Rh(cod)Cl]₂(μ-dpnapy) **2** (0.051 g, 0.06 mmol), and the resulting mixture left to stir for 30 min. By addition of hexane compound **1** precipitated in nearly quantitative yield (0.068 g, 0.114 mmol) (Found: C, 61.35; H, 5.35; Cl, 6.05; N, 4.80; P, 5.30. Calc. for C₃₀H₃₁ClN₂PRh: C, 61.20; H, 5.30; Cl, 6.00; N, 4.75; P, 5.25%). IR (Nujol, CsI): ν(Rh-Cl) 288 cm⁻¹.

[Rh(cod)Cl]₂(μ-dpnapy) **2**. **Procedure (a)**. A dichloromethane solution (40 cm³) of dpnapy (0.042 g, 0.122 mmol) and [Rh(cod)Cl]₂ (0.060 g, 0.122 mmol) was stirred for 20 min. The initially yellow colour turned orange. By addition of hexane compound **2** precipitated as a yellow-orange solid. It was filtered off and washed with diethyl ether. Recrystallization from dichloromethane-diethyl ether (1:2) (30 cm³) gave **2** as orange crystals in 90% yield (0.092 g, 0.1098 mmol).

Procedure (b). Solid [Rh(cod)Cl]₂ (0.063 g, 0.127 mmol) was added to a dichloromethane (30 cm³) solution of [Rh(cod)(dpnapy)Cl] **1** (0.150 g, 0.254 mmol). Soon the yellow starting solution turned orange. The resulting mixture was left to stir for *ca.* 10 min, then hexane (40 cm³) was added inducing the precipitation of **2**. Yield 0.187 g, 88% (Found: C, 54.85; H, 5.25; Cl, 8.65; N, 3.40. Calc. for C₃₈H₄₃Cl₂N₂PRh₂: C, 54.65; H, 5.20; Cl, 8.50; N, 3.35%). IR (Nujol, CsI): ν(Rh-Cl) 287 and 267 cm⁻¹. M, 800 (CHCl₃) (calc. 835).

[Rh(CO)(μ-dpnapy)Cl]₂ **3**. **Procedure (a)**. The addition of solid dpnapy (0.090 g, 0.263 mmol) to a benzene solution (50 cm³) of [Rh(CO)₂Cl]₂ (0.051 g, 0.131 mmol) produced immediately a change in colour from orange to lemon-yellow. The reaction mixture was left to stir for *ca.* 10 min, during which time compound **3** precipitated as an orange solid. Diethyl ether (40 cm³) was then added to complete the precipitation. The orange solid was filtered off, washed with diethyl ether (3 × 5 cm³) and dried *in vacuo* (yield 95%).

Procedure (b). Carbon monoxide was bubbled through a dichloromethane solution of compound **1** (0.055 g, 9.34 mmol) for 15 min. After this time the bubbling was stopped, diisopropyl ether (30 cm³) was added and the resulting mixture left to stand for 24 h. During this time compound **3** precipitated as orange crystals in nearly quantitative yield (Found: C, 54.20; H, 3.80; Cl, 7.10; N, 4.95. Calc. for C₂₃H₁₉ClN₂OPRh: C, 54.30; H, 3.75; Cl, 7.00; N, 5.50%). IR (CsI, Nujol): ν(CO) 1975; ν(Rh-Cl) 291 cm⁻¹.

Reaction of Compound 1 with CO.—See preparation of complex **3**, procedure (b).

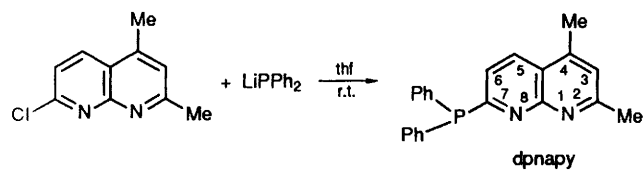
Reaction of Compound 2 with CO.—Compound **2** (0.040 g, 4.78 mmol) was dissolved in dichloromethane (20 cm³) and CO bubbled through the solution. Immediately the colour changed from orange to lemon-yellow. While maintaining the flow of CO, hexane (40 cm³) was added inducing the precipitation of a light yellow solid. The mother-liquor was pipetted off and the solid washed with diethyl ether (3 × 5 cm³) and dried under an atmosphere of CO. The yellow solid at room temperature (*r.t.*) slowly transforms into compound **3** and unidentified products. IR (Nujol, CsI): ν(CO) 2070vs and 2007vs; ν(Rh-Cl) 257 and 247 cm⁻¹.

X-Ray Data Collection and Structure Refinement.—Orange crystals of [Rh(CO)(μ-dpnapy)Cl]₂·2CH₂Cl₂ **3** were obtained by slow evaporation from a dichloromethane-heptane solution. Diffraction data were collected on a Siemens R3m/V automatic four-circle diffractometer, using graphite-monochromated Mo-Kα radiation. To avoid the loss of solvent a selected crystal was covered with fast-setting acrylic glue and used for intensity data collection. Lattice parameters were obtained from least-squares refinement of the setting angles of 25 reflections in the range 15 ≤ 2θ ≤ 30°. Information concerning the conditions of crystallographic data collection and structure refinement is summarized in Table 4. From the 4450 unique intensities collected up to 50° at room temperature by the ω-2θ scan method, 3718 were assumed as observed [*I* ≥ 3σ(*I*)]. Lorentz polarization and φ-scan absorption corrections¹³ were applied to the intensity data. The structures were solved by standard Patterson methods and subsequently completed by Fourier recycling. The full-matrix least-squares refinement was based on *F*_o. All non-hydrogen atoms were refined anisotropically. All hydrogen atoms were set in calculated positions and refined as riding atoms, with a common thermal parameter. Convergence was achieved at *R* = 0.039, *R*' = 0.042. The weighting scheme used in the last refinement cycles was *w* = [σ²(*F*_o) + 0.000 364(*F*_o)²]⁻¹. Solutions, refinements and drawings were performed with the SHELXT-PLUS system.¹⁴ The final geometrical calculations were performed with the PARST program.¹⁵

Additional material available from the Cambridge Crystallographic Data Centre comprises H-atom coordinates, thermal parameters, and remaining bond lengths and angles.

Results and Discussion

Synthesis of 7-Diphenylphosphino-2,4-dimethyl-1,8-naphthyridine.—Treatment of a thf solution of lithium diphenylphosphide with the stoichiometric amount of 7-chloro-2,4-dimethyl-1,8-naphthyridine yields a dark red-violet solution



Scheme 1

Table 1 Proton and ^{13}C NMR data for dpnapy^a

^1H NMR ^b					
H ³	H ⁵	H ⁶	2-Me	4-Me	Ph
7.19	8.14	7.20	2.73	2.62	7.47 (m, 4 H) 7.36 (m, 6 H)
	[$J(\text{H}^5\text{H}^6)$ 8.4] [$J(\text{H}^5\text{P})$ 2.02]				
^{13}C NMR ^c					
C ³	C ⁵	C ⁶	2-Me	4-Me	Ph
123.70	132.29	124.16	25.60	17.95	134.48 ^d 128.88 ^e [$J(\text{CP})$ 26.18] 128.62 ^f
		[$J(\text{C}^6\text{P})$ 15.6]			[$J(\text{CP})$ 20.13]

^a In CDCl_3 , 297 K, chemical shifts (δ) referred to SiMe_4 and coupling constants (J) in Hz. ^b At 200.13 MHz. ^c At 50.323 MHz. Quaternary carbons were found at δ 168.74, 162.98, 145.41, 136.22 [$J(\text{CP})$ 11.6 Hz] and 119.42 were not assigned. ^d meta. ^e ortho. ^f para.

Table 2 Phosphorus-31 NMR data^a

Compound	T/K	δ	$J(\text{PRh})/\text{Hz}$
dpnapy ^b	295	-1.1	149
1 ^c	295	30.52	149
2 ^c	295	28.50	149
	195	35.9	149
		24.1	149
3 ^b	295	41.4	171

^a At 80.015 MHz, chemical shifts (δ) referred to external H_3PO_4 . ^b In CDCl_3 . ^c In CD_2Cl_2 .

from which 7-diphenylphosphino-2,4-dimethyl-1,8-naphthyridine was obtained (Scheme 1) in 55% yield after purification by column chromatography (see Experimental section).

The ligand dpnapy is a white crystalline solid, stable for a long time even in air, but its solution must be handled under nitrogen because the corresponding phosphine oxide is easily formed. It dissolves well in benzene and dichloromethane but only sparingly in diethyl ether. Its structure was determined by a combination of elemental analysis, IR, ^1H , ^{31}P and ^{13}C NMR spectral data (Tables 1 and 2). In the IR spectrum, along with the bands related to the phenyl rings, two strong bands, attributable to the C=N naphthyridine skeletal stretching modes, are observed at 1580 and 1610 cm^{-1} . The ^{31}P - $\{^1\text{H}\}$ NMR spectrum consists of a single sharp resonance at δ -1.12. Owing to the presence of several overlappings, particularly in the aromatic region, the assignments of the ^1H and ^{13}C NMR spectra required the combination of one- and two-dimensional techniques. The proton spectrum exhibits two singlets at δ 2.62 (3 H) and 2.73 (3 H), assigned, on the basis of reference data,^{16,17} to 4- and 2-Me, respectively, and a well resolved doublet of doublets at δ 8.14 (1 H) due to H⁵. The assignment, as in Table 1, was then completed and confirmed by two-dimensional ^1H COSY and ^1H NOESY measurements. In particular the COSY spectrum helped partially to resolve the complex multiplets between δ 7.6 and 7.3 (assigned to the protons of the two phenyl rings) and to attribute H⁶ at δ 7.20.

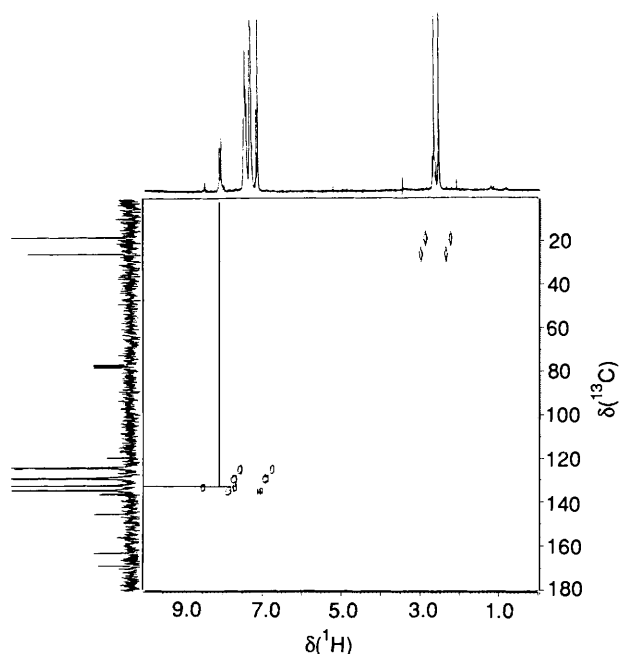
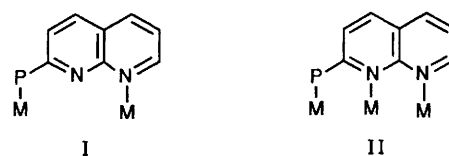


Fig. 1 Counter plot of the two-dimensional ^{13}C - ^1H (200.13 MHz, CDCl_3 , 297 K) inverse correlation spectrum for dpnapy. The correlation between H⁵ and C⁵ is indicated



Scheme 2

The observation in the NOESY spectrum of NOE effects between the signals at δ 2.73 (2-Me) and 7.19 (H³), 2.62 (4-Me) and 8.14 (H⁵), 8.14 (H⁵) and 7.20 (H⁶) unambiguously confirmed the attribution of the proton resonances. Knowing the ^1H NMR spectrum, the assignment of the protonated carbons was straightforward on the basis of two-dimensional ^1H - ^{13}C correlation spectroscopy (Fig. 1). In the counter plot only the protons coupled to ^{13}C nuclei appear as doublets [$\delta(^1\text{H})$ being the centre of the doublet on the horizontal scale] lying in rows which correspond to the relative $\delta(^{13}\text{C})$ on the vertical scale. For simplicity the normal horizontal and vertical projections obtained in this measurement have been substituted with the ^1H and ^{13}C - $\{^1\text{H}\}$ NMR spectra of dpnapy.

The dpnapy ligand, like 1,8-naphthyridine (napy) and 2-(diphenylphosphino)pyridine (dppy), is characterized by a rigid skeleton which constrains the phosphorus and nitrogen atoms in fixed and nearly coplanar position. As can be seen from Scheme 2 the present ligand may display, beside the coordination modes of the napy and dppy fragments, the binucleating (I) and the trinucleating (II) modes. Of course the nature of the metal will determine the co-ordination mode. Hard metals will co-ordinate preferentially to nitrogen, soft metals to phosphorus, although the presence of methyl in *ortho* position to N(1) increases the softness of the latter. In addition the asymmetric disposition of the co-ordination sites in dpnapy could produce asymmetrical heteropolynuclear assemblies of metal ions not accessible with symmetrical tridentate ligands.

Reactions with Rhodium Complexes.—The reaction of $[\{\text{Rh}(\text{cod})\text{Cl}\}_2]$ with dpnapy yields different products depending on the molar ratio of the reactants. From the 1:2 reaction in dichloromethane solution the mononuclear complex $[\text{Rh}(\text{cod})(\text{dpnapy})\text{Cl}]$ **1** is isolated in nearly quantitative yield. It is a yellow air-stable solid which dissolves easily in almost all

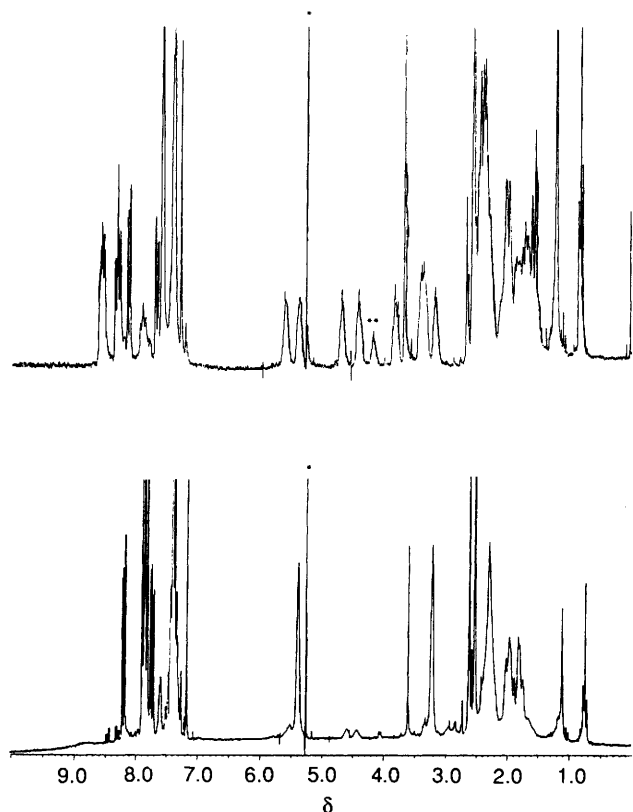


Fig. 2 Proton NMR spectra (200.13 MHz, CD_2Cl_2) of complexes **1** at 215 K (below) and **2** at 295 K (above): * indicates impurities and solvent peaks; ** olefinic cod protons due to $[\{\text{Rh}(\text{cod})\text{Cl}\}_2]$

solvents. Its solutions are stable in air only for a short time owing to the formation of the naphthyridine phosphine oxide and $[\{\text{Rh}(\text{cod})\text{Cl}\}_2(\mu\text{-dpnapy})]$ **2**. Phosphorus co-ordination to rhodium is evidenced by the ^{31}P NMR spectrum which shows at r.t. a doublet at δ 30.5 [$J(\text{Rh-P}) = 149$ Hz]. The ^1H and ^{13}C NMR spectra are temperature dependent. At r.t. in the ^1H NMR spectrum no resonances are observed for the cod olefinic protons suggesting that a dynamic process occurs in solution. By lowering the temperature (215 K) this process is frozen and two signals appear at δ 5.4 (m) and 3.2 (m) (Fig. 2). Accordingly, at r.t. no signals are detectable for the olefinic cod carbons in the ^{13}C NMR spectrum, whereas at 215 K two signals emerge at δ 106.5 [dd, $J(\text{Rh-C}) = 12$, $J(\text{C-P}) = 7$ Hz] and at 71.6 [d, $J(\text{Rh-C}) = 12$ Hz]. Since the NMR-active ligand atoms *trans* to co-ordinated phosphines couple to the ^{31}P atoms with relatively large 3J value, the assignment of the resonance at lower frequencies to the olefinic cod carbons *trans* to co-ordinated dpnapy is easily made (Table 3). By measuring the two-dimensional ^{13}C - ^1H correlation spectrum (215 K) the corresponding protons are unambiguously identified.

The observed fluxionality may be explained in terms of (i) rotation of the diolefin *via* $\eta^4\text{-}\eta^2\text{-}\eta^4$ isomerization, (ii) Berry pseudo-rotation *via* a five-co-ordinate intermediate. This last mechanism has often been invoked to explain the fluxional behaviour for some square-planar cycloocta-1,5-diene d^8 complexes. The major path involves the formation of stereochemically labile five-co-ordinate species formed *via* an intermolecular association equilibrium^{18,19} or *via* intramolecular attack.^{20,21} A similar associative mechanism, involving the formation of a five-co-ordinated species *via* intramolecular attack of N(8) on the rhodium atom, may be also invoked to explain the fluxionality of **1**. This assumption receives additional support from the observation that a similar fluxionality is not observed in the complex $[\{\text{Rh}(\text{cod})\text{Cl}\}_2(\mu\text{-dpnapy})]$ **2** (see below) where dpnapy acts as a bridging bidentate ligand.

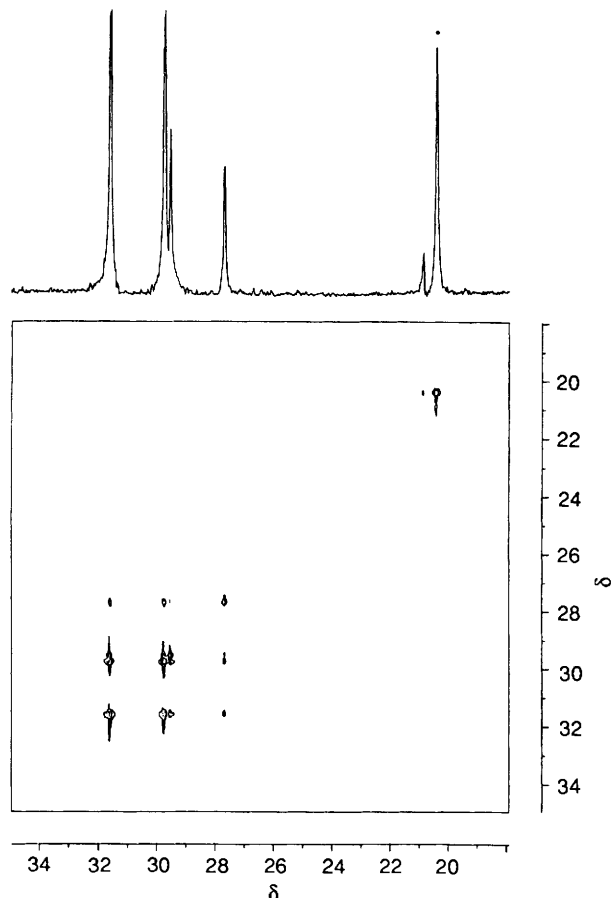


Fig. 3 Counter plot of the two-dimensional ^{31}P (81.015 MHz, CD_2Cl_2 , at 297 K) chemical exchange spectrum for complex **1**. The cross-peaks between the two doublets indicate the exchange $\mathbf{1} \rightleftharpoons \mathbf{2}$; * due to dpnapy oxide

The appearance of the ^1H and ^{13}C low-temperature spectra of complex **1** is consistent with a C_s structure instead of the expected C_1 . To judge from **2** (see below) we can reasonably assume that the rigid asymmetric placement of the dpnapy ligand should lead to significant shifts for the cod alkene nuclei. We then suggest that some fluxionality, not frozen at 215 K, averages the cod atoms above and below the co-ordination plane. The preservation of all the coupling constants [$J(\text{P-Rh})$, $J(\text{C-Rh})$, $J(\text{C-P})$] rules out any dissociative process, suggesting that the observed averaging is due to the fast rotation of the co-ordinated dpnapy about the Rh-P bond, which gives rise to a pseudo-plane of symmetry.

Finally following by ^{31}P NMR spectroscopy the evolution of a dichloromethane solution of complex **1** at 295 K we observed a third slower dynamic process. The spectrum of **1** newly dissolved contains the species $[\{\text{Rh}(\text{cod})\text{Cl}\}_2(\mu\text{-dpnapy})]$ **2** in ratio 4.5:1. On standing the amount of **2** increases and after a few days at 0 °C the ratio **1**:**2** becomes 1:1. The process is reversible; by adding to this sample free dpnapy the ratio **1**:**2** goes back to 4.5:1. The slow equilibration $\mathbf{1} \rightleftharpoons \mathbf{2}$ with the participation of free dpnapy has been monitored by running the two-dimensional ^{31}P chemical exchange spectrum (NOESY sequence) of **1** (Fig. 3).

The binuclear complex $[\{\text{Rh}(\text{cod})\text{Cl}\}_2(\mu\text{-dpnapy})]$ **2** is the product of reaction of $[\{\text{Rh}(\text{cod})\text{Cl}\}_2]$ with dpnapy when the molar ratio 1:1 is used. It can alternatively be obtained by addition of an equivalent amount of $[\{\text{Rh}(\text{cod})\text{Cl}\}_2]$ to **1**. Complex **2** is an orange crystalline solid, soluble in benzene and chlorinated solvents, but insoluble in acetone and alcohols, and air stable both in the solid state and in solution. Concentration-dependent conductivity measurements carried out in chloroform solutions of **2** show that no ionic species are

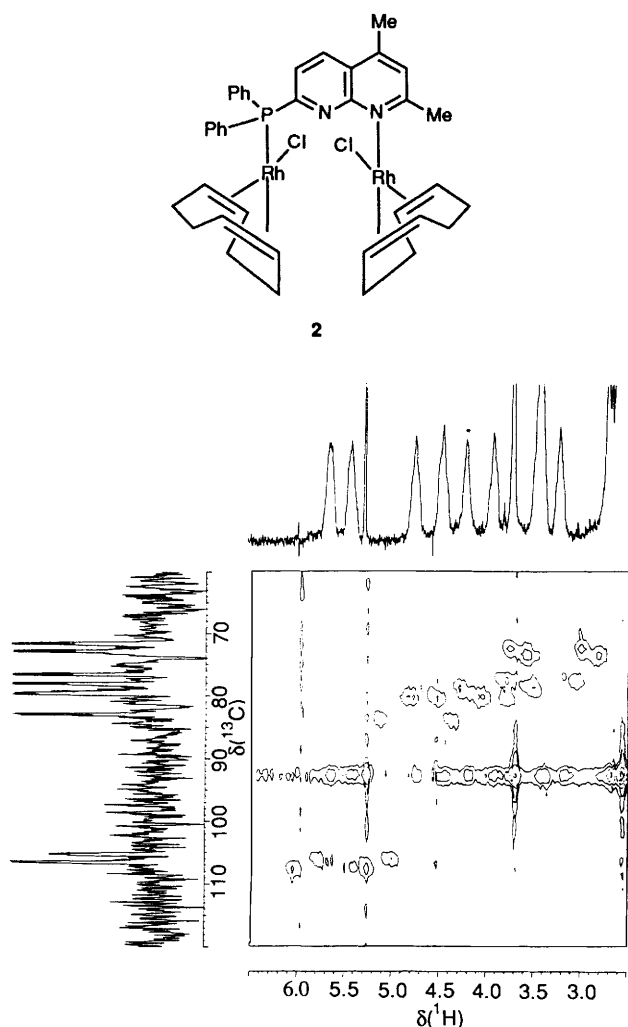


Fig. 4 Section of the counter plot of the two-dimensional ^{13}C - ^1H (200.13 MHz, CD_2Cl_2 , at 295 K) inverse correlation spectrum for complex **2**. Eight doublets are observed in the counter plot due to the olefinic cod protons plus a doublet due to $[\{\text{Rh}(\text{cod})\text{Cl}\}_2]$ (*) at δ 4.17. Artefacts appears at $F_1 = 0$. Horizontal and vertical projections are section of the ^1H and ^{13}C NMR spectra, respectively

Table 3 Proton and ^{13}C NMR data^a for complexes **1** and **2**

(a) ^1H NMR				
Complex	Me_2	Me_4	$\text{CH}(\text{cod})$	$\text{CH}_2(\text{cod})$
1 ^b	2.66	2.54	5.4, ^c 3.2	1.8, 2.5
2 ^d	3.66	2.55	5.60, ^e 5.38, ^e 4.68, 4.40, 3.82, 3.37, ^e 3.17	1.8, 2.4
(b) ^{13}C NMR ^f				
1 ^b	26.5	19.1	106.5 (7), 71.6	33.8, 29.7
2 ^g	31.9	18.7	106.5 (7), 105.2 (7), 82.9, 79.6, 78.1, 76.5, 72.8, 71.6	28, 35

^a In CD_2Cl_2 , at 200.13 (^1H) and 50.323 (^{13}C) MHz, chemical shifts (δ) referred to SiMe_4 , coupling constants (J) in Hz. ^b At 215 K. ^c *trans* to P. ^d At 295 K. ^e Intensity 2 H. ^f All the olefinic carbons of the co-ordinated cod exhibit $J(\text{C}-\text{Rh}) = 12$ Hz, $J(\text{CP})$ in parentheses. ^g At 253 K.

present. Its IR spectrum shows unchanged the bands associated with the internal modes of the naphthyridine rings and consequentially was not indicative of the co-ordination mode of

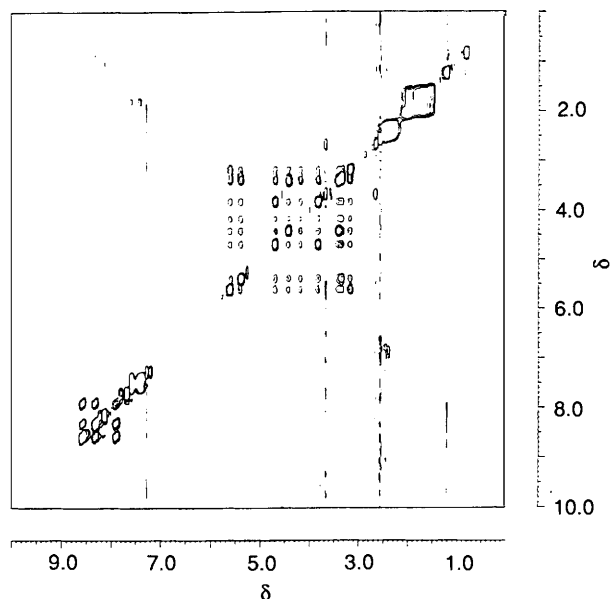
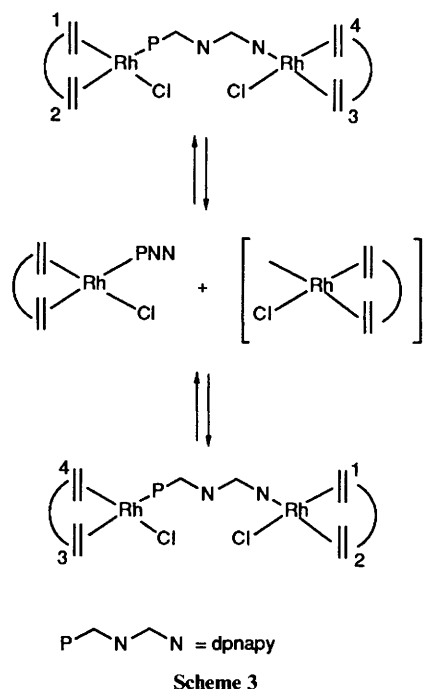


Fig. 5 Counter plot of the two-dimensional ^1H (200.13 MHz, CD_2Cl_2 , 295 K) chemical exchange spectrum (NOESYPH sequence) of complex **2**. Only peaks due to chemical exchange (negative peaks) have been plotted

dpnapy. The dimeric structure shown with the *dpnapy* ligand bridging two $\text{Rh}(\text{cod})\text{Cl}$ moieties by P and N(1) atoms has been assigned on the basis of the NMR data.

The ^1H and ^{13}C NMR spectra of complex **2** (Figs. 2 and 4) show eight different absorptions for the olefinic cod protons and carbons, thus indicating a structure of C_1 symmetry containing two cod molecules in a chemical and magnetic non-equivalence. The complete assignment of such complex spectra is not trivial and would require various NMR measurements. For the purpose of this work we have concentrated on defining the overall structure of the molecule and assigning some relevant resonances (Table 3). The carbon-proton connectivity has been obtained by two-dimensional ^{13}C - ^1H correlation measurements (Fig. 4). As explained above, on the basis of the observation of ^{13}C - ^{31}P couplings, the two ^{13}C lower frequencies at δ 106.5 and 105.2, which correlated with the ^1H resonances at δ 5.60 and 5.38, have been attributed to the olefinic cod carbons and protons, respectively, *trans* to phosphorus. The resonance at δ 4.17 in the proton spectrum and the corresponding ^{13}C resonance at about δ 79 are not due to impurity, being involved in the dynamics of **2** (see later). On the basis of literature data²²⁻²⁴ and reactivity considerations they have been assigned to the olefinic proton and carbon of $[\{\text{Rh}(\text{cod})\text{Cl}\}_2]$. The analysis of the NMR data in Tables 1 and 3 affords further evidence for a dimeric structure of **2**. Comparing the ^1H and ^{13}C findings for free *dpnapy*, **1** and **2** we notice that the methyl group closer to N(1) is very sensitive to the co-ordination mode of *dpnapy*. As expected no major changes are observed between the relative data for free *dpnapy* (^1H , δ 2.73; ^{13}C , 25.60) and **1** (^1H , δ 2.66; ^{13}C , 26.5) whereas a strong downfield shift is observed for those of **2** (^1H , δ 3.66; ^{13}C , 31.9). The bidentate co-ordination mode **I** (see Scheme 2) brings the methyl group close to the rhodium atom and results in an NMR shift for this group attributed to the magnetic anisotropy of the metal.²² Consistent with this formulation the ^{31}P NMR spectrum of **2** shows a doublet at δ 28.5 [$J(\text{Rh}-\text{P}) = 149$ Hz].

The NMR findings also indicate that complex **2** is involved in several dynamic processes. A simple inspection of the ^1H spectrum (Fig. 2) shows all olefinic cod-proton signals are rather broad. This might be due to: (i) a slow dynamic process, (ii) the presence of several couplings for each proton. To settle this question we have run a two-dimensional ^1H chemical exchange spectrum (NOESYPH sequence) of **2** which allows



one to differentiate positive NOE from chemical exchange. The result shown in Fig. 5 evidences that a slow exchange occurs at r.t. among (a) all the olefinic cod protons, (b) all the olefinic cod protons of **2** and the species at δ 4.17, (c) the 2-Me proton signal of **2** (δ 3.66) and that at δ 2.66 due to the 2-Me protons of **1**. A two-dimensional proton-exchange experiment run at lower temperature (253 K) shows that the cod dynamics and exchange involving the 2-Me group (*i.e.* the equilibration $\mathbf{2} \rightleftharpoons \mathbf{1}$) are frozen. Although we cannot exclude the possibility of several independent dynamic processes which occur at similar rate, this complex fluxionality of **2** can be explained by the equilibration $\mathbf{2} \rightleftharpoons \mathbf{1}$ via the intermediacy of **1** and $[\{\text{Rh}(\text{cod})\text{Cl}\}_2]$ as depicted in Scheme 3.

Finally a faster dynamic process involving complex **2** can be monitored by ^{31}P NMR spectroscopy. The spectra recorded in the temperature range 295–195 K are reported in Fig. 6. At 295 K the spectrum consists of two doublets at δ 30.52 and 28.50, due to **1** and **2**, respectively. The doublet of **2** coalesces at 223 K and reappears as a couple of doublets (δ 35.9 and 24.1) at 193 K. Unfortunately no further NMR data are available because at this temperature the poor solubility of **2** and the viscosity of the solvent prevent the measurement of the ^{13}C NMR spectrum and analysis of the ^1H NMR spectrum. On the basis of the ^{31}P NMR findings, since the observed couplings are the same [$^1J(\text{Rh}-\text{P}) = 149$ Hz] in the mean and frozen spectrum of **2** we suggest that the low-temperature species might be stereoisomers in rapid exchange at r.t.

Reaction of dpnapy with $[\{\text{Rh}(\text{CO})_2\text{Cl}\}_2]$.—The addition of dpnapy to a benzene solution of $[\{\text{Rh}(\text{CO})_2\text{Cl}\}_2]$ affords a lemon-yellow solution which slowly turns orange while CO evolution is observed. Work-up of the resulting mixture (see Experimental section) leads to the complex $[\{\text{Rh}(\text{CO})(\mu\text{-dpnapy})\text{Cl}\}_2]$ **3**, as an orange precipitate in high yield. Examination of IR spectra (r.t., C_6H_6) reveals that, in the reaction of dpnapy with $[\{\text{Rh}(\text{CO})_2\text{Cl}\}_2]$, *cis*-dicarbonyl-rhodium species are initially formed as evidenced by two strong bands at 2007 and 2070 cm^{-1} . These on standing are replaced by a stronger one at 1975 cm^{-1} , consistent with the formation of **3**. Compound **3** is an air-stable microcrystalline solid the low solubility of which prevents full spectral analysis. The IR spectrum (Nujol) indicates the presence of one terminal carbonyl group (1975 cm^{-1}) and one terminal chlorine (291

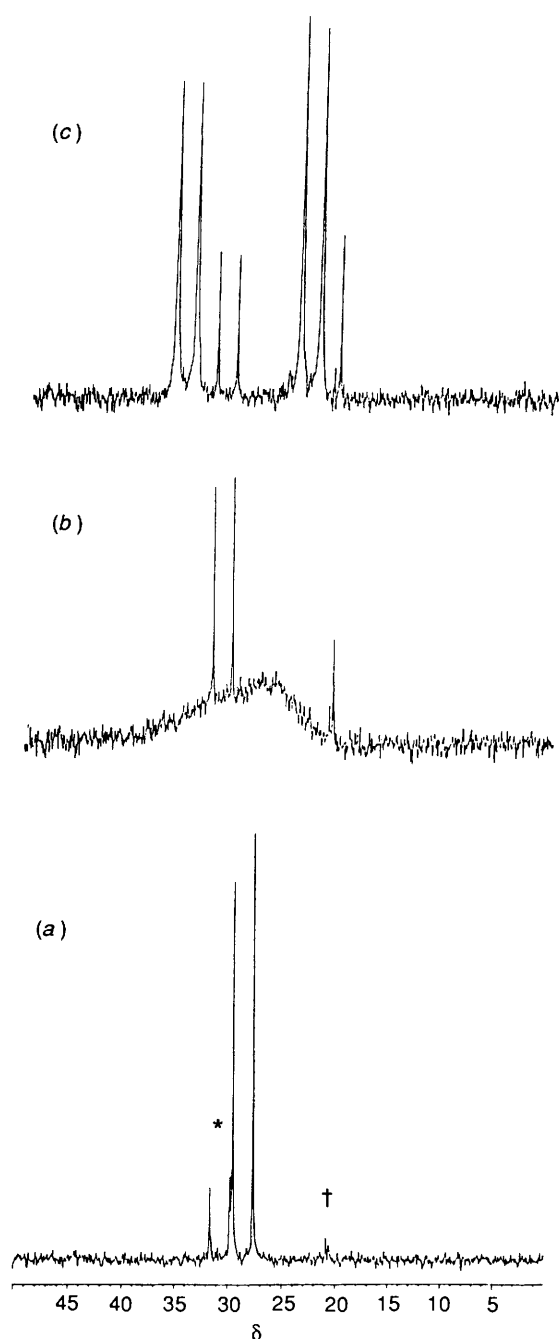


Fig. 6 ^{31}P NMR spectra (81.015 MHz, CD_2Cl_2) for complex **2** at (a) 295, (b) 233 and (c) 193 K; * due to traces of complex **1** and † of dpnapy oxide

cm^{-1}), while the $^{31}\text{P}-\{^1\text{H}\}$ NMR spectrum (Table 2) consists of a doublet centred at δ 41.4 [$^1J(\text{Rh}-\text{P}) = 171$ Hz]. Complex **3** can alternatively be obtained by treating **1** or **2** with carbon monoxide.

Reaction of Complex 2 with CO.—Treatment of complex **2** (see Experimental section) leads to the formation of a yellow solid which slowly transforms into **3** and other unidentified products. The IR spectrum of the yellow solid shows two strong $\nu(\text{CO})$ absorptions at 2007 and 2070 cm^{-1} characteristic of a *cis*-dicarbonyl species. All attempts better to characterize it failed because it consists, as shown by ^1H , ^{13}C and ^{31}P NMR variable-temperature spectra, of a mixture of compounds.

Crystal and Molecular Structure of $[\{\text{Rh}(\text{CO})(\mu\text{-dpnapy})\text{Cl}\}_2] \cdot 2\text{CH}_2\text{Cl}_2$ **3.**—The molecular structure of complex **3**,

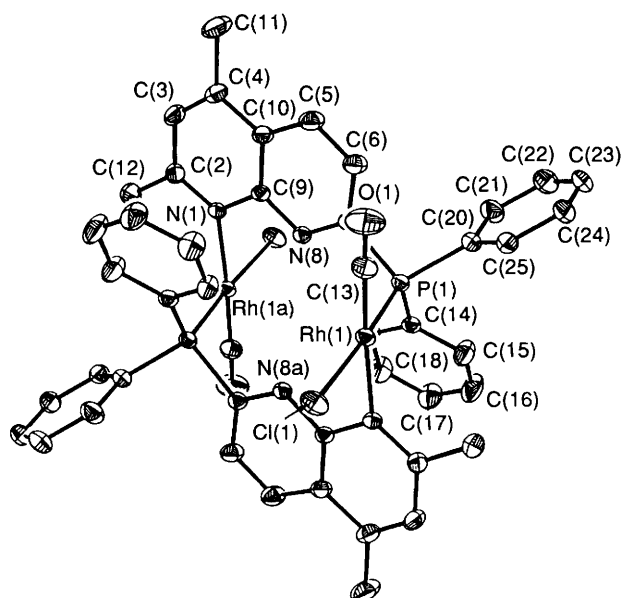


Fig. 7 View of complex 3 with the numbering scheme. Thermal ellipsoids are drawn at 30% probability. Hydrogen atoms are omitted for clarity

Table 4 Crystallographic data for $[\text{Rh}_2(\text{CO})_2(\mu\text{-dpnapy})_2\text{Cl}_2] \cdot 2\text{CH}_2\text{Cl}_2$ 3

Formula	$\text{C}_{48}\text{H}_{42}\text{Cl}_6\text{N}_4\text{O}_2\text{P}_2\text{Rh}_2$
<i>M</i>	1187.4
Space group	<i>P</i> $\bar{1}$
<i>a</i> /Å	11.706(1)
<i>b</i> /Å	11.836(2)
<i>c</i> /Å	11.989(2)
α /°	62.28(1)
β /°	63.27(1)
γ /°	63.88(1)
<i>U</i> /Å ³	1256.0(3)
<i>Z</i>	1
<i>D_c</i> /g cm ⁻³	1.570
<i>F</i> (000)	596
Crystal size/mm	0.12 × 0.15 × 0.40
μ (Mo-K α)/cm ⁻¹	10.7
2 θ range/°	3–54
No. of collected reflections	4787
No. of unique reflections	4450
No. of observed reflections ^a	3718
<i>R</i> ^b	0.039
<i>R</i> ^c	0.042
<i>S</i> ^d	1.69

^a With $I \geq 3\sigma(I)$. ^b $R = \sum(|F_o| - |F_c|)/\sum|F_o|$. ^c $R' = [\sum(|F_o| - |F_c|)^2/\sum w|F_o|^2]^{1/2}$. ^d Goodness of fit = $[\sum w(|F_o| - |F_c|)^2/(N_o - N_p)]^{1/2}$ where N_o , N_p = number of observations and parameters.

including the atomic numbering scheme, is illustrated in Fig. 7; the two CH_2Cl_2 molecules of crystallization have been omitted for clarity. Crystal data, selected bond distances and angles, and atomic coordinates are reported in Tables 4, 5 and 6 respectively.

The structure consists of two $\text{Rh}(\text{CO})\text{Cl}$ fragments symmetrically bridged by two dpnapy ligands, arranged in a head-to-tail fashion, to form a dinuclear complex in which the CO and Cl groups are located in a *cis* position. The bridging function of the ligand is realized through phosphorus and N(1) atoms. Each rhodium atom has a distorted square-planar geometry, being surrounded by N(1) and P atoms of two different molecules, with Cl and CO acting as terminal groups. The Rh–Cl, Rh–N and Rh–C(CO) distances are very similar to

Table 5 Final atomic coordinates ($\times 10^4$) for complex 3 with standard deviations (e.s.d.s) in parentheses

Atom	<i>x</i>	<i>y</i>	<i>z</i>
Rh(1)	1 020(1)	1 919(1)	2 388(1)
Cl(1)	2 989(1)	2 338(1)	2 056(1)
Cl(2)	4 610(3)	914(3)	6 068(3)
Cl(3)	3 149(4)	3 723(4)	4 933(7)
P(1)	–793(1)	1 381(1)	2 897(1)
O(1)	–608(4)	4 667(4)	2 367(5)
N(1)	–2 333(3)	–53(3)	7 841(3)
C(2)	–3 032(4)	138(5)	9 011(4)
C(3)	–4 028(5)	1 332(5)	9 120(5)
C(4)	–4 318(5)	2 372(5)	8 056(5)
C(10)	–3 545(4)	2 208(4)	6 777(4)
C(5)	–3 689(5)	3 184(5)	5 570(5)
C(6)	–2 931(5)	2 918(4)	4 422(5)
C(7)	–1 989(4)	1 659(4)	4 466(4)
N(8)	–1 817(3)	709(3)	5 584(3)
C(9)	–2 591(4)	980(4)	6 730(4)
C(11)	–5 392(6)	3 646(6)	8 172(6)
C(12)	–2 704(5)	–973(6)	10 203(5)
C(13)	20(5)	3 576(5)	2 403(5)
C(14)	–482(4)	–325(4)	3 051(4)
C(15)	–137(6)	–568(5)	1 891(5)
C(16)	259(7)	–1 846(6)	1 891(6)
C(17)	320(6)	–2 904(5)	3 029(6)
C(18)	–22(6)	–2 694(5)	4 186(5)
C(19)	–419(5)	–1 407(4)	4 192(4)
C(20)	–1 820(4)	2 354(4)	1 799(4)
C(21)	–2 951(5)	2 042(5)	2 067(5)
C(22)	–3 726(5)	2 764(7)	1 227(6)
C(23)	–3 373(6)	3 809(6)	112(6)
C(24)	–2 272(5)	4 137(5)	–168(5)
C(25)	–1 485(4)	3 405(4)	665(4)
C(26)	3 498(9)	2 086(11)	5 269(16)

Table 6 Selected interatomic distances (Å) and angles (°) for complex 3 with e.s.d.s in parentheses

Rh(1)–Cl(1)	2.390(2)	Rh(1)–P(1)	2.225(1)
Rh(1)–C(13)	1.792(5)	Rh(1)–N(1a)	2.125(3)
P(1)–C(7)	1.846(4)	O(1)–C(13)	1.162(6)
N(1)–C(2)	1.336(6)	N(1)–C(9)	1.372(5)
C(2)–C(3)	1.399(6)	C(2)–C(12)	1.490(3)
C(3)–C(4)	1.349(6)	C(4)–C(10)	1.443(7)
C(4)–C(11)	1.497(7)	C(10)–C(5)	1.397(6)
C(10)–C(9)	1.398(5)	C(5)–C(6)	1.356(7)
C(6)–C(7)	1.404(5)	C(7)–N(8)	1.320(5)
N(8)–C(9)	1.359(5)		
Rh(1)···N(8a)	3.924(2)	Rh(1)···Rh(1a)	5.932(2)
Cl(1)–Rh(1)–P(1)	174.2(1)	Cl(1)–Rh(1)–C(13)	91.7(2)
P(1)–Rh(1)–C(13)	90.6(2)	Cl(1)–Rh(1)–N(1a)	85.1(1)
P(1)–Rh(1)–N(1a)	93.0(1)	C(13)–Rh(1)–N(1a)	173.7(2)
Rh(1)–P(1)–C(7)	109.2(2)	Rh(1)–P(1)–C(14)	115.0(1)
C(7)–P(1)–C(14)	108.7(2)	C(2)–N(1)–C(9)	117.9(3)
C(2)–N(1)–Rh(1a)	124.1(2)	C(9)–N(1)–Rh(1a)	117.5(3)
N(1)–C(2)–C(3)	121.7(4)	N(1)–C(2)–C(12)	117.3(4)
C(3)–C(2)–C(12)	121.0(4)	C(2)–C(3)–C(4)	122.4(5)
C(3)–C(4)–C(10)	116.9(4)	C(3)–C(4)–C(11)	122.5(5)
C(10)–C(4)–C(11)	120.6(4)	C(4)–C(10)–C(5)	124.8(4)
C(4)–C(10)–C(9)	118.2(4)	C(5)–C(10)–C(9)	117.0(4)
C(10)–C(5)–C(6)	120.2(4)	C(5)–C(6)–C(7)	119.0(4)
P(1)–C(7)–C(6)	118.9(3)	P(1)–C(7)–N(8)	117.8(3)
C(6)–C(7)–N(8)	122.8(4)	C(7)–N(8)–C(9)	117.7(3)
N(1)–C(9)–C(10)	122.8(4)	N(1)–C(9)–N(8)	114.0(3)
C(10)–C(9)–N(8)	123.2(3)	Rh(1)–C(13)–O(1)	177.6(4)

Symmetry code: a $-x, -y, 1 - z$.

those found in related compounds and do not require special comments. The Rh–P bond distance (2.225 Å) is shorter than that found in the complex $[\text{Rh}_2\{\mu\text{-(Ph}_2\text{P)}_2\text{C}_3\text{H}_3\text{N}\}_2(\text{CO})_2\text{(MeOH)Cl}]\text{PF}_6$ ^{25b} (mean value 2.347 Å). This shortening can

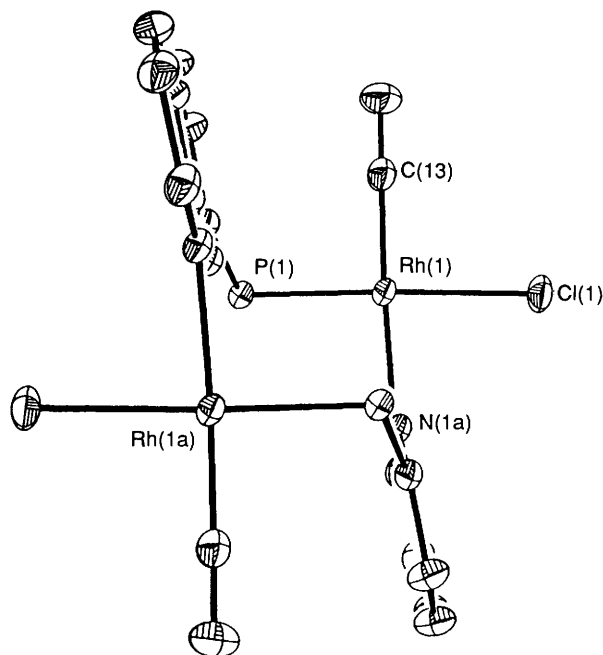


Fig. 8 Partial view of complex 3 showing the arrangement of the ligand around the rhodium atoms

be attributed to the smaller *trans* effect of chlorine with respect to that of the phosphorus atoms.²⁶

The Rh(1) atom is 0.091(1) Å out of the least-squares plane through Cl(1), C(13), P(1) and N(1a), the largest deviation from planarity being 0.242(5) Å for C(13). As can be deduced from Fig. 8 the symmetry forces the rhodium co-ordination planes to be parallel, but depending on the *cis* disposition of the CO and Cl groups they do not face each other; indeed the Rh(1)···Rh(1a) distance [5.932(2) Å] is greater than the interplane separation (4.98 Å). The naphthyridine planes are forced to be parallel by crystallographic symmetry too, and are separated by 2.15 Å. The *cis* arrangement of the CO and Cl groups determines the almost perpendicular directions of the Rh(1)–P(1) and Rh(1)–N(1a) bonds and different lone-pair bonding directions of the two unco-ordinated dpnapy nitrogen atoms [N(8) and N(8a)].

Similar structural features have been found in the metallocycle *cis,cis*-[Pt[μ-(Ph₂P)₂C₅H₃N]Cl₂]₂²⁷ where the *cis* disposition of the chlorine atoms imposes a similar assembly of the molecule. Such an assembly prevents the co-ordination of other metal ions in the central cavity. On the contrary, in the metallocycle [Rh(CO)[μ-(Ph₂P)₂C₅H₃N]Cl]₂²⁵ the *trans* configuration of the Rh(CO)Cl unit allows the co-ordination of a SnCl⁺ in the central cavity.²⁸

Acknowledgements

We thank the Ministero per l'Università e la Ricerca Scientifica e Tecnologica for financial support.

References

- 1 A. L. Balch, L. A. Fosset, J. K. Nagle and M. M. Olmstead, *J. Am. Chem. Soc.*, 1988, **110**, 6732.
- 2 A. L. Balch, *Pure Appl. Chem.*, 1988, **60**, 555 and refs. therein.
- 3 A. L. Balch, V. J. Catalano, M. A. Chatfield, J. K. Nagle, M. M. Olmstead and P. E. Reedy, jun., *J. Am. Chem. Soc.*, 1991, **113**, 1252 and refs. therein.
- 4 (a) G. Bruno, S. Lo Schiavo, E. Rotondo, P. Piraino and F. Faraone, *Organometallics*, 1987, **6**, 2502 and refs. therein; (b) E. Rotondo, S. Lo Schiavo, G. Bruno, C. G. Arena, R. Gobetto and F. Faraone, *Inorg. Chem.*, 1989, **28**, 2944; (c) G. Bruno, S. Lo Schiavo, E. Rotondo, C. G. Arena and F. Faraone, *Organometallics*, 1989, **8**, 886; (d) S. Lo Schiavo, E. Rotondo, G. Bruno and F. Faraone, *Organometallics*, 1991, **10**, 1613.
- 5 M. Munakata, M. Maekawa, S. Kitagawa, M. Adachi and H. Masuda, *Inorg. Chim. Acta*, 1990, **167**, 181; A. Tiripicchio, M. Tiripicchio Camellini, R. Uson, L. A. Oro, M. A. Ciriano and F. Viguri, *J. Chem. Soc., Dalton Trans.*, 1984, 125 and refs. therein.
- 6 J. P. Collin, A. Jouaiti, J. P. Sauvage, W. C. Kaska, M. A. McLoughlin, N. L. Keder, W. T. A. Harrison and G. D. Stucky, *Inorg. Chem.*, 1990, **29**, 2238; A. T. Baker, W. R. Tikkanen, W. C. Kaska and P. C. Ford, *Inorg. Chem.*, 1984, **23**, 3254.
- 7 M. A. Ciriano, B. E. Villaroya and L. A. Oro, *Inorg. Chim. Acta*, 1986, **120**, 43.
- 8 J. P. Farr, M. M. Olmstead and A. L. Balch, *Inorg. Chem.*, 1983, **22**, 1229; *J. Am. Chem. Soc.*, 1980, **102**, 6654.
- 9 G. Giordano and R. H. Crabtree, *Inorg. Synth.*, 1979, **19**, 218.
- 10 J. A. McCleverty and G. Wilkinson, *Inorg. Synth.*, 1966, **8**, 211.
- 11 A. Mangini and M. Colonna, *Gazz. Chim. Ital.*, 1943, **73**, 323.
- 12 G. A. Morris, *Magn. Reson. Chem.*, 1986, **24**, 3H.
- 13 A. C. T. North, D. C. Phillips and F. S. Mathews, *Acta Crystallogr., Sect. A*, 1968, **24**, 351.
- 14 SHELXL PLUS, version 3.4, Siemens Analytical X-ray Instruments, Madison, WI, 1989.
- 15 M. Nardelli, *Comput. Chem.*, 1983, **7**, 95.
- 16 W. W. Paudler and T. J. Kress, *J. Heterocycl. Chem.*, 1967, **4**, 284 and refs. therein.
- 17 A. C. Boicelli, R. Danieli, A. Mangini, L. Lunari and G. Placucci, *J. Chem. Soc., Perkin Trans. 2*, 1973, 1024.
- 18 E. Anzueta, M. A. Garralda, R. Hernandez, L. Ibarlucea, E. Pinilla and M. A. Monge, *Inorg. Chim. Acta*, 1991, **185**, 211.
- 19 C. Volger, K. Vrieze and A. P. Praat, *J. Organomet. Chem.*, 1968, **14**, 429.
- 20 H. El-Amouri, A. A. Bahsoun and J. A. Osborn, *Polyhedron*, 1988, **7**, 2035.
- 21 P. Imhoff, R. Van Asselt, C. J. Elsevier, M. C. Zoutberg and C. H. Stam, *Inorg. Chim. Acta*, 1991, **184**, 73 and refs. therein.
- 22 K. Vrieze, C. Volger and A. P. Praat, *J. Organomet. Chem.*, 1968, **14**, 185.
- 23 R. Bonnaire and N. Platzer, *J. Organomet. Chem.*, 1976, **104**, 107.
- 24 D. E. Chebi and I. P. Rothwell, *Organometallics*, 1990, **9**, 2948 and refs. therein.
- 25 (a) F. E. Wood, M. M. Olmstead and A. L. Balch, *J. Am. Chem. Soc.*, 1983, **105**, 6332; (b) F. E. Wood, J. Hvoslief and A. L. Balch, *J. Am. Chem. Soc.*, 1983, **105**, 6986.
- 26 M. J. Bennet and P. B. Donaldson, *Inorg. Chem.*, 1977, **16**, 655.
- 27 F. E. Wood, J. Hvoslief, H. Hope and A. L. Balch, *Inorg. Chem.*, 1984, **23**, 4309.
- 28 A. L. Balch, H. Hope and F. E. Wood, *J. Am. Chem. Soc.*, 1985, **107**, 6936.

Received 24th January 1992; Paper 2/00396A